



Title	Spatial dynamics of action potentials estimated by dendritic Ca ²⁺ signals in insect projection neurons
Author(s)	Ogawa, Hiroto; Mitani, Ruriko
Citation	Biochemical and Biophysical Research Communications, 467(2), 185-190 https://doi.org/10.1016/j.bbrc.2015.10.021
Issue Date	2015
Doc URL	http://hdl.handle.net/2115/62889
Type	article (author version)
File Information	Ogawa&Mitani_manuscript.pdf



[Instructions for use](#)

Spatial dynamics of action potentials estimated by dendritic Ca²⁺ signals in insect projection neurons

Hiroto Ogawa^{a,*} and Ruriko Mitani^b

^aDepartment of Biological Sciences, Faculty of Science, Hokkaido University, Sapporo
060-0810, Japan

^bGraduate School of Life Science, Hokkaido University, Sapporo 060-0810, Japan

*Correspondence to: Hiroto Ogawa

Department of Biological Sciences, Faculty of Science, Hokkaido University,

Kita 10-jyo, Nishi 8, Kita-ku, Sapporo 060-0810, Japan

Phone/Fax: +81-11-706-3525

E-mail: hogawa@sci.hokudai.ac.jp

ABSTRACT

The spatial dynamics of action potentials, including their propagation and the location of spike initiation zone (SIZ), are crucial for the computation of a single neuron.

Compared with mammalian central neurons, the spike dynamics of invertebrate neurons remain relatively unknown. Thus, we examined the spike dynamics based on single spike-induced Ca^{2+} signals in the dendrites of cricket mechanosensory projection neurons, known as giant interneurons (GIs). The Ca^{2+} transients induced by a synaptically evoked single spike were larger than those induced by an antidromic spike, whereas subthreshold synaptic potentials caused no elevation of Ca^{2+} . These results indicate that synaptic activity enhances the dendritic Ca^{2+} influx through voltage-gated Ca^{2+} channels. Stimulation of the presynaptic sensory afferents ipsilateral to the recording site evoked a dendritic spike with higher amplitude than contralateral stimulation, thereby suggesting that alteration of the spike waveform resulted in synaptic enhancement of the dendritic Ca^{2+} transients. The SIZ estimated from the spatial distribution of the difference in the Ca^{2+} amplitude was distributed throughout the right and left dendritic branches across the primary neurite connecting them in GIs.

Keywords

Calcium imaging; dendrite; insect neuron; laterality; spike initiation zone; spike propagation

Abbreviations

EPSP, excitatory postsynaptic potential; GI, giant interneuron; LI, laterality index; OGB-1, Oregon Green 488 BAPTA-1; ROI, region of interest; SIZ, spike initiation zone; TAG, terminal abdominal ganglion; VGCC, voltage-gated Ca^{2+} channel.

Highlights

- ◆ Synaptic inputs enhance single spike-induced Ca^{2+} transients in GI dendrites.
- ◆ Single spike-induced Ca^{2+} transients in dendrites reflect the input distribution.
- ◆ Height, not half-width, of dendritic spikes is increased by synaptic activation.
- ◆ SIZ estimated from Ca^{2+} response laterality is distributed on bilateral dendrites.

1. Introduction

The spatial dynamics of action potentials, including where the spikes originate and how they propagate within the neuronal structure, are crucial for the computation of a single neuron. In general, it is understood that action potentials are initially generated at the axonal hillock close to the cell body, but numerous studies of dendritic excitability in mammalian central neurons have demonstrated the complex dynamics of spikes, such as back-propagation into dendrites and local dendritic spikes [1-3]. Compared with vertebrate neurons, there have been relatively few studies of the spike dynamics in invertebrate neurons. In invertebrate neurons that are unipolar neurons, the action

potentials are considered to initiate along the primary neurite connecting the axon and dendritic branches, where the membrane contains high-density voltage-gated ion channels that are involved in spike generation [4]. However, multiple spike initiation zones (SIZs) have been identified in invertebrate neurons, and the spike initiation site can be altered by the location and strength of the synaptic inputs [5-7]. The dendritic distribution of the action potentials and the spike propagation dynamics are not known; thus, to clarify these issues, we examined the spike dynamics based on single spike-induced Ca^{2+} signals in the dendrites of projection neurons known as giant interneurons (GIs) in crickets.

Eight pairs of ascending projection neurons have been identified as GIs in the field cricket, *Gryllus bimaculatus* [8]. The GIs have a soma and arborize into distinct dendritic branches within the terminal abdominal ganglion (TAG). Their characteristic dendritic shape allows easy identification of the individual cells. The GIs project their large-diameter axons to the thoracic and cephalic ganglia through a connective nerve cord contralateral to the soma [8-10]. The GIs receive excitatory synaptic inputs from sensory afferents of the mechanoreceptive hairs on the cerci, which are sensory organs that comprise a pair of antenna-like appendages at the rear of the cricket's abdomen [11].

The GIs process and convey sensory information about the direction and dynamics of air particle displacement [12-15]. The directional sensitivity of GIs is based primarily

on the relative positions of their dendrites within the afferent map of the mechanosensory afferents [16]. In addition, Ca^{2+} imaging studies have demonstrated that the overall directional tuning depends on the spatial distribution of synapses in the complex geometry of the dendritic arbors [17,18]. A probable location of the SIZ in GIs is at or near the junction between the axon and primary neurite [12], but electrophysiological recordings obtained from multiple sites in GIs have demonstrated that the direction of spike propagation might possibly be altered by synaptic activity [19]. Thus, to describe the dendritic dynamics of action potentials in GIs, we simultaneously recorded single spikes and the dendritic Ca^{2+} transients when the GIs were stimulated synaptically or antidromically. Based on the spatial distribution of laterality in the single spike-induced Ca^{2+} signals, we then estimated the dendritic zone capable of initiating action potentials in GIs.

2. Materials and Methods

2. 1. Preparation

Experiments were performed using laboratory-bred, adult male crickets (*Gryllus bimaculatus*). The guidelines of the Institutional Animal Care and Use Committee of the National University Corporation, Hokkaido University, Japan, specify no particular requirements for the treatment of insects in experiments. After an incision along the dorsal midline of the abdomen, the gut, internal reproductive organs, and surrounding

fat were removed to expose the TAG. To remove the sheath from the TAG, a piece of filter paper soaked in 10% type XIV protease (Sigma-Aldrich, St Louis, MO, USA) was placed on the dorsal side for 1 min. After washing with isotonic saline, a preparation that comprised the fourth and terminal abdominal ganglia, abdominal connective nerves, cercal nerves, and cerci was isolated from the body and whole-mounted in a glass recording chamber.

2. 2. Electrophysiology

The GI membrane potential were recorded intracellularly with a glass microelectrode (30–50 M Ω) filled with 150 mM potassium acetate and 2 mM Oregon Green 488 BAPTA-1 (OGB-1) potassium salt (Thermo Fisher Scientific, Waltham, MA USA). Using an MMO-203 micromanipulator (Narishige, Tokyo, Japan), the intracellular electrode was inserted into the dendritic shaft or primary neurite of GIs, which was confirmed by fluorescent imaging using an Axiovert100 inverted microscope (Carl Zeiss Microscopy GmbH, Jena, Germany). A pair of hook electrodes positioned under the abdominal connective nerve cords was used to provide antidromic stimulation, where a single short pulse (pulse duration 50 μ s) was applied to the connective nerve cord. For synaptic stimulation, a single pulse was applied to the left or right cercal nerve with two pairs of hook electrodes. The stimulus intensity was adjusted to a subthreshold level, which evoked excitatory postsynaptic potentials (EPSPs), or to a suprathreshold

level to generate a single action potential. Electrophysiological signals were digitized at 20 kHz with a Powerlab 4s analog-to-digital converter (ADInstruments, Dunedin, New Zealand) and analyzed using Chart v.7 software (ADInstruments).

2. 3. *Dye loading and Ca²⁺ imaging*

The fluorescent Ca²⁺ indicator (OGB-1) was loaded iontophoretically into GIs for 5 min through a glass microelectrode at a hyperpolarizing current of 3 nA. Fluorescence images were observed using an inverted microscope (Zeiss) equipped with a Fluar 10×, 0.5 NA dry objective lens (Zeiss), with illumination from a XBO 75 w Xenon arc lamp (Zeiss), which had a stabilized power supply, and a 480/20 band-pass filter for the excitation of OGB-1. GI Ca²⁺ signals were measured in fluorescence images captured through a FT510 dichroic mirror and 535/45 band-pass filter. A series of images was acquired at 30 Hz and 256 × 256 pixels using an ORCA-ER digital cooled-CCD camera (Hamamatsu Photonics, Hamamatsu, Japan) attached to the microscope. Fluorescence intensities obtained from each image were background corrected and the average value was determined for each square or polygonal region of interest (ROI) in recordings. To obtain time-course images of the changes in fluorescence for several ROIs, the mean fluorescence intensities from four trials were plotted as a function of time. Changes in the cytosolic Ca²⁺ concentration were calculated as $\Delta F/F$: [$\Delta F/F = (F - F_0)/F_0$], where F_0 is the corrected pre-stimulus fluorescence intensity. Relative fluorescence ($\Delta F/F$)

images were processed and displayed in pseudo-color using AQUACOSMOS/Ratio software (Hamamatsu Photonics).

2. 4. Data analysis

We used the peak value of $\Delta F/F$ during a period of 500 ms after stimulation as the magnitude of a Ca^{2+} signal. To analyze the bilateral difference in the Ca^{2+} signals, we calculated a laterality index (LI), which is similar to the standard metric of ocular dominance [20-23]. The LI was determined using the following formula:

$$LI = \frac{R_{axon} - R_{soma}}{R_{axon} + R_{soma}}$$

where R_{axon} and R_{soma} represent the magnitudes of the Ca^{2+} responses to synaptic stimulation of the axon and soma sides of cercal nerves, respectively. To compare the waveform of single action potentials, we measured the amplitude and half-width of individual spikes. The spike amplitude was defined as the difference between the resting potential immediately before stimulation and the spike peak, and the half-width was defined as the duration of the period when the membrane potential was depolarized above half of the spike amplitude. We also measured the spike delay, which we defined as the time interval between the stimulus artifact and the spike peak.

3. Results and Discussion

3. 1. Ca^{2+} elevation induced by a single action potential

Transient Ca^{2+} elevation following the single action potentials evoked by both antidromic and synaptic stimulation was detected at the primary neurite and distal dendrites in GIs (Fig. 1A). The Ca^{2+} transients induced by the synaptically evoked spike were larger than those induced by the antidromic spike (Fig. 1B). The difference in the amplitude of the Ca^{2+} transients between the synaptic and antidromic stimulations was more pronounced in the distal dendrites than that in the primary neurite ($p = 0.0291$ for primary neurites; $p = 0.0005$ for distal dendrites, Wilcoxon signed-rank test). This result implies that synaptic activation enhanced the spike-induced Ca^{2+} elevation in dendrites.

The subthreshold synaptic stimulation that evoked EPSP caused no significant change in the fluorescence of OGB-1 (Fig. 1C; $p = 0.6822$, compared to the maximum value in $\Delta F/F$ during the pre-stimulation period, Wilcoxon signed-rank test), thereby indicating that subthreshold synaptic activation induced no increase in the cytosolic Ca^{2+} . By contrast, when the action potential was generated by synaptic stimulation with an intensity slightly above the firing threshold, the cytosolic Ca^{2+} level increased greatly in the whole dendrites (Fig. 1D; $p = 0.0001$ for primary neurite, $p = 0.0001$ for distal dendrites, Wilcoxon signed-rank test). The cercal-to-GIs synapses are thought to be cholinergic [24,25], but it is likely that influx through the nicotinic receptors or release from internal stores mediated by muscarinic receptors do not contribute to the Ca^{2+} signals in GIs. These results also suggest that the Ca^{2+} signals observed in the GIs were attributable entirely to the Ca^{2+} influx through the voltage-gated Ca^{2+} channels

(VGCCs), which is consistent with the results of previous studies that used tetanic stimulation [19,26]. The larger depolarization caused by the dendritic spike is probably more likely to activate the VGCCs, thereby enhancing the Ca^{2+} influx in the dendrites.

3. 2. Relationship between the recording location of dendritic Ca^{2+} responses and response laterality

The difference in the single spike-induced Ca^{2+} transients via VGCCs due to antidromic and synaptic stimulation suggests that the synaptically evoked action potentials differed in terms of their waveform compared with the antidromic spikes. If this is the case, then it is possible that the dendritic Ca^{2+} signals induced by a single spike also depend on the location of the activated synaptic sites. Thus, we selectively stimulated the right or left cercal nerves, which contain mechanoreceptor afferents that project to the ipsilateral hemisphere of the TAG [27,28], and we compared the single spike-induced Ca^{2+} transients between the stimulated sides. The distal dendrites mainly responded to stimulation of the cercal nerve ipsilateral to the recorded region, whereas the primary neurites connecting the bilateral dendritic branches did not differ in terms of the Ca^{2+} response (Fig. 2A). Laterality in the dendritic Ca^{2+} response to synaptic stimulation was observed in GIs 9-3, 10-2, and 10-3, which bilaterally arborize their dendritic branches in the TAG (Fig. 2B). These results demonstrate that the single spike-induced Ca^{2+} influx via VGCCs depends on the location of the activated synaptic

sites, which suggests that the waveforms of the dendritic spikes were altered by the spatial pattern of synaptic activation.

3. 3. Difference in the waveforms of synaptically evoked spikes between the stimulated sides

Next, we compared the synaptically evoked spikes between the stimulated sides in terms of their waveforms. There was no difference in the action potentials recorded at the primary neurite with axon and soma side stimulation. However, the recordings from the distal dendrites on the soma side indicated that stimulation of the soma side evoked a greater action potential than stimulation of the axon side or antidromic stimulation (Fig. 3A). In all types of GIs with arborized bilateral dendrites, the spikes evoked by stimulation of the cercal nerve ipsilateral to the recording site were significantly larger than those evoked by stimulation of the contralateral side (Fig. 3C, $p = 2.62E-13$, Mann–Whitney U test). By contrast, there was no significant difference in the half-width of the individual spikes between the stimulated sides ($p = 0.7594$).

One of the possible mechanisms responsible for synaptic enlargement of the dendritic spike height is additional depolarization of the action potential back-propagating from the SIZ into the dendrites by the EPSPs. The SIZ of GIs is considered to be located at or near the junction site between the axon and the primary neurite that links the dendritic arborizations [12]. In computational models of insect

neurons, including cricket GIs, the SIZ is typically located on the primary neurite close to the axon [18,29,30]. However, a previous study showed that antidromic stimulation combined with subthreshold synaptic stimulation does not enhance the dendritic spikes or induce Ca^{2+} elevation to the same extent as that induced by synaptically evoked spikes [19]. Furthermore, the lack of difference in the half-width of the dendritic spikes with ipsi- and contralateral stimulation suggests that the simple addition of a synaptic potential to the back-propagating spike is not capable of enhancing the action potentials in dendrites.

It is also possible that the action potential itself is generated at the dendritic shaft close to the activated input sites, thereby causing greater depolarization. In some arthropod neurons, multiple SIZs have been identified, each of which generates action potentials independently [5-7,31]. The recordings from the dendrites of GIs 10-2 and 9-3 often indicated action potentials with double peaks at different amplitudes (Fig. 3B), thereby suggesting the presence of multiple SIZs [31]. Furthermore, the action potentials evoked by stimulation ipsilateral to the recording site had a shorter delay than those evoked by contralateral side stimulation (Fig. 3C; $p = 0.0002$, Mann–Whitney U test). These results demonstrate that the action potentials were generated at neurites close to the activated synaptic sites, thereby supporting multiple SIZs. The components of the ionic currents that produce the dendritic spikes in GIs remain unknown [32], but the prominent Ca^{2+} transients observed at the dendrites strongly suggest that

voltage-dependent Ca^{2+} currents contribute to dendritic spike generation. It is possible that GI dendrites have more excitable membrane properties, which may allow GIs to generate doublet spikes that augment amount of information [33].

3. 4. Spatial distribution of laterality in the dendritic Ca^{2+} responses

If the increase in the spike height underlies the synaptic enhancement of the dendritic Ca^{2+} signals, then differences in the Ca^{2+} transients with partial synaptic stimulation will reflect the shift in location of the initiation site depending on the synaptic activity. Therefore, to estimate the distribution of SIZs in GIs, we examined the spatial distribution of the bilateral difference in the dendritic Ca^{2+} transients induced by synaptic stimulation on the right and left sides. We calculated the LI for each ROI based on the amplitude of the Ca^{2+} transients for various cellular regions in GI 10-2 (see Materials and Methods) and we superimposed the color map on the morphology of GI 10-2 (Fig. 4A). Across the midline, opposite lateralities were clearly visible in the dendrites, whereas the neurite connecting the bilateral dendritic branches and axons exhibited little or no laterality.

If the dendritic Ca^{2+} transients depend solely on the spike height, then action potentials can be generated in the area between the locations of the positive and negative maximum values. This is because the bilateral difference in the spike height will reach a peak at the generation site for spikes evoked by synaptic simulation on the

left or right sides. Figure 4B shows that the difference in the Ca^{2+} amplitude along the right and left dendritic shafts connected by the primary neurite produced a sigmoidal curve, where the positive peak was obtained on the axon side of the dendrite at a distance of 250 μm and the negative peak was obtained on the soma side at 150 μm from the intersection point across the midline. Thus, it is possible that the dendritic spikes can be generated in the area between these positions within GI 10-2. The dendritic shaft can probably initiate the synaptically evoked action potentials, which will propagate to the primary neurite and to the other side of dendrites.

The dendritic Ca^{2+} signals induced by air current stimuli exhibit low heterogeneity in their response properties such as directionality [18,20], so the action potentials are probably initiated in a narrow zone in the neurite. However, the GIs even exhibited spatial differences in the directional selectivity of the dendritic Ca^{2+} signals in response to an air current [17,18,34]. Therefore, fluctuations in the SIZ may facilitate the compartmentalization of Ca^{2+} accumulation, thereby leading to selective adaptation to a specific stimulus [34,35].

Acknowledgments

This study was supported by funding for H.O. from the Japan Science and Technology Agency (JST), Precursory Research for Embryonic Science and Technology (PRESTO), and JSPS KAKENHI Grant Number 26440176 to H.O.

References

- [1] M. Häusser, N. Spruston, G.J. Stuart, Diversity and dynamics of dendritic signaling, *Science*. 290 (2000) 739–744.
- [2] M. London, M. Häusser, Dendritic computation, *Annu. Rev. Neurosci.* 28 (2005) 503–32.
- [3] N. Spruston, Pyramidal neurons: dendritic structure and synaptic integration, *Nat. Rev. Neurosci.* 9 (2008) 206–221.
- [4] C. Kuehn, C. Duch. Putative excitatory and putative inhibitory inputs are localised in different dendritic domains in a *Drosophila* flight motoneuron, *Eur. J. Neurosci.* 37 (2013) 860–875.
- [5] D. Mellon Jr., Dendritic initiation and propagation of spikes and spike bursts in a multimodal sensory interneuron: the crustacean parasol cell, *J. Neurophysiol.* 90 (2003) 2465–2477.
- [6] J.B. Thuma, W.E. White, K.H. Hobbs, S.L. Hooper, Pyloric neuron morphology in the stomatogastric ganglion of the lobster, *Panulirus interruptus*, *Brain Behav. Evol.* 73 (2009) 26–42.
- [7] N. Daur, F. Nadim, W. Stein, Regulation of motor patterns by the central spike-initiation zone of a sensory neuron, *Eur. J. Neurosci.* 30 (2009) 808–822.

- [8] K. Hirota, Y. Sonoda, Y. Baba, T. Yamaguchi, Distinction in morphology and behavioral role between dorsal and ventral groups of cricket giant interneurons, *Zool. Sci.* 10 (1993) 705–709.
- [9] B. Mendenhall, R.K. Murphey, The morphology of cricket giant interneurons, *J. Neurobiol.* 5 (1974) 565–580.
- [10] G.A. Jacobs, R.K. Murphey, Segmental origins of the cricket giant interneuron system, *J. Comp. Neurol.* 265 (1987) 145–157.
- [11] J.P. Bacon, R.K. Murphey, Receptive fields of cricket giant interneurons are related to their dendritic structure, *J. Physiol.* 352 (1984) 601–623.
- [12] G.A. Jacobs, J.P. Miller, R.K. Murphey, Cellular mechanisms underlying directional sensitivity of an identified sensory interneuron, *J. Neurosci.* 6 (1986) 2298–2311.
- [13] J.P. Miller, F.E. Theunissen, G.A. Jacobs, Representation of sensory information in the cricket cercal sensory system. I. Response properties of the primary interneurons, *J. Neurophysiol.* 66 (1991) 1680–1689.
- [14] F.E. Theunissen, J.P. Miller, Representation of sensory information in the cricket cercal sensory system. II. Information theoretic calculation of system accuracy and optimal tuning curve widths of four primary interneurons, *J. Neurophysiol.* 66 (1991) 1690–1703.

- [15] F. Theunissen, J.C. Roddey, S. Stufflebeam, H. Clague, J.P. Miller, Information theoretic analysis of dynamical encoding by four primary sensory interneurons in the cricket cercal system, *J. Neurophysiol.* 75 (1996) 1345–1376.
- [16] G.A. Jacobs, F.E. Theunissen, Extraction of sensory parameters from a neural map by primary sensory interneurons, *J. Neurosci.* 20 (2000) 2934–2943.
- [17] H. Ogawa, Y. Baba, K. Oka, Directional sensitivity of dendritic calcium responses to wind stimuli in cricket giant interneurons, *Neurosci. Lett.* 358 (2004) 185–188.
- [18] H. Ogawa, G.I. Cummins, G.A. Jacobs, K. Oka, Dendritic design implements algorithm for synaptic extraction of sensory information, *J. Neurosci.* 28 (2008) 4592–4603.
- [19] H. Ogawa, Y. Baba, K. Oka, Direction of action potential propagation influences calcium increase in distal dendrites of the cricket giant interneurons, *J. Neurobiol.* 53 (2002) 44–56.
- [20] U.C. Dräger, Receptive fields of single cells and topography in mouse visual cortex, *J. Comp. Neurol.* 160 (1975) 269–290.
- [21] J.A. Gordon, M.P. Stryker, Experience-dependent plasticity of binocular responses in the primary visual cortex of the mouse, *J. Neurosci.* 16 (1996) 3274–3286.
- [22] J.L. Hanover, Z.J. Huang, S. Tonegawa, M.P. Stryker, Brain-derived neurotrophic factor overexpression induces precocious critical period in mouse visual cortex, *J. Neurosci.* 19 (1999) RC40.

- [23] B. Scholl, J.J. Pattadkal, G.A. Dilly, N.J. Priebe, B.V. Zemelman, Local integration accounts for weak selectivity of mouse neocortical parvalbumin interneurons, *Neuron* 87 (2015) 424–436.
- [24] M.R. Meyer, G.R. Reddy, Muscarinic and nicotinic cholinergic binding sites in the TAG of the cricket (*Acheta domestica*), *J. Neurochem.* 45 (1985) 1101–1112.
- [25] O. Yono, H. Aonuma, Cholinergic neurotransmission from mechanosensory afferents to giant interneurons in the terminal abdominal ganglion of the cricket *Gryllus bimaculatus*, *Zool. Sci.* 25 (2008) 517–525.
- [26] H. Ogawa, Y. Baba, K. Oka, Spike-dependent calcium influx in dendrites of the cricket giant interneuron, *J. Neurobiol.* 44 (2000) 45–56.
- [27] S. Paydar, C.A. Doan, G.A. Jacobs, Neural mapping of direction and frequency in the cricket cercal sensory system, *J. Neurosci.* 19 (1999) 1771–1781.
- [28] G.A. Jacobs, F. Theunissen, Functional organization of a neural map in the cricket cercal sensory system, *J. Neurosci.* 16 (1996) 769–784.
- [29] P.W. Jones, F. Gabbiani, Logarithmic compression of sensory signals within the dendritic tree of a collision-sensitive neuron, *J. Neurosci.* 32 (2012) 4923–4934.
- [30] C. Günay, F.H. Sieling, L. Dharmar, W.H. Lin, V. Wolfram, R. Marley, R.A. Baines, A.A. Prinz, Distal spike initiation zone location estimation by morphological simulation of ionic current filtering demonstrated in a novel model of an identified *Drosophila* motoneuron, *PLoS Comput. Biol.* 11 (2015) e1004189.

- [31] K.A. Killian, J.P. Bollins, C.K. Govind, Anatomy and physiology of neurons composing the commissural ring nerve of the cricket, *Acheta domesticus*, J. Exp. Zool. 286 (2000) 350–366.
- [32] P. Kloppenburg, M. Hörner, Voltage-activated currents in identified giant interneurons isolated from adult crickets *Gryllus bimaculatus*, J. Exp. Biol. 201 (1998) 2529–2541.
- [33] Z.N. Aldworth, A.G. Dimitrov, G.I. Cummins, T. Gedeon, J.P. Miller, Temporal encoding in a nervous system, PLoS Comput. Biol. 7 (2011) e1002041.
- [34] H. Ogawa, K. Oka, Direction-Specific adaptation in neuronal and behavioral responses of an insect mechanosensory system, J Neurosci. 35 (2015) 11644–11655.
- [35] J. Prešern, J.D. Triplehorn, J. Schul, Dynamic dendritic compartmentalization underlies stimulus-specific adaptation in an insect neuron, J. Neurophysiol. 113 (2015) 3787–3797.

Figure legends

Fig. 1.

Ca²⁺ signals induced by synaptic and antidromic stimulation. (A, C) Dendritic Ca²⁺ signals induced by single action potentials evoked by antidromic or synaptic stimulation (A) and induced by sub- or suprathreshold synaptic stimulation (C). Gray lines show Ca²⁺ signals recorded at the distal dendrite and primary neurite close to the axon during each trial, and black lines show the averaged signal from four trials. Dashed lines indicate the timing of stimulation. The superimposed upper red traces show four action potentials (A, C) or excitatory postsynaptic potentials (EPSPs) (C), which were recorded simultaneously with the Ca²⁺ signals. The upper left cartoon in each panel shows the stimulation paradigm and the intracellular recording site. Lower left drawings indicate the morphology of the GIs and the regions for recording the Ca²⁺ signals. Horizontal scale bars = 2 ms (upper) and 1 s (lower); vertical scale bars = 20 mV (upper) and 1% in $\Delta F/F$. (B, D) Differences in the peak values of the Ca²⁺ transients between antidromic and synaptic spikes (B) and between EPSP and action potentials (D). Lines connecting open circles correspond to the mean of four trials using individual samples (12 pairs of measurements in 10 neurons for B: two neurons for GI 8-1, two neurons for GI 9-3, six neurons for GI 10-2; 19 pairs of measurements in 15 neurons for D: six neurons for GI 8-1, one neuron for GI 9-2, three neurons for GI 9-3, and five

neurons for GI 10-2). Columns show the mean values. * $p < 0.05$, *** $p < 0.001$, Wilcoxon signed-rank test.

Fig. 2.

Laterality in the dendritic Ca^{2+} responses to synaptic stimulation. (A) Typical Ca^{2+} response in different dendritic regions to electrical stimulation of uni- and bilateral sensory afferents. The upper pseudo-color images show dendritic Ca^{2+} elevation induced by single action potentials in GI 10-2 and ROIs for the lower traces. Each trace indicates the averaged signal from four trials measured at the distal dendrites on the axon (red regions of interest, ROIs) and soma sides (blue ROIs), and at the primary neurites connecting the bilateral dendritic branches (green ROIs). Horizontal scale bars = 1 s; vertical scale bars = 1% in $\Delta F/F$. The upper left cartoon shows the stimulation paradigm. (B) Scatter plots showing the relationship between the amplitude of dendritic Ca^{2+} signals in the recorded location and the stimulation side. The Ca^{2+} responses were measured at two different dendritic regions on the axon (red) and soma sides (blue) in GIs 9-3 (4 measurements in three neurons), 10-2 (12 measurements in 10 neurons), and 10-3 (2 measurements in two neurons). Dotted line represents $Y = X$ line. The upper drawings indicate the morphology of the GIs and ROIs of the Ca^{2+} signals.

Fig. 3.

Differences in the waveforms and delay of dendritic spikes between the stimulated sides.

(A) Typical waveform of action potentials recorded at the primary neurite (upper) and distal dendrite (lower) in GI 10-2. Each trace indicates the single action potentials evoked by synaptic stimulation of the cercal nerve on the soma or axon side and by antidromic stimulation of the ascending axon within the connective nerve cord.

Horizontal scale bar = 2 ms; vertical scale bar = 25 mV. (B) Double-peaked action potentials recorded at the dendritic branch of GI 9-3. Four traces have been superimposed, which were aligned at their leading edges. These spikes were evoked by synaptic stimulation on the side ipsilateral to the recording site. Horizontal scale bar = 2 ms; vertical scale bar = 10 mV. Inset cartoons in (A) and (B) show the stimulation paradigms and intracellular recording sites. (C) Pooled data for the amplitude,

half-width, and delay to peak for the single action potentials evoked by unilateral synaptic stimulation. The action potentials were recorded repeatedly at various sites on the dendrites of GIs (four measurements in one neuron for GI 8-1, 16 measurements in three neurons for GI 9-3, 21 measurements in six neurons for GI 10-2). Columns and error bars indicate mean \pm S.E.M. *** $p < 0.001$, Mann–Whitney U test.

Fig. 4.

Spatial distribution of bilateral differences in the dendritic Ca^{2+} responses to synaptic stimulation in GI 10-2. (A) Color maps indicating the spatial distribution of LI (see

Materials and Methods) calculated from the magnitude of Ca^{2+} signals. The colors of the tiles superimposed on the fluorescent image of GI 10-2 represent the mean of LI as indicated by the color codes on the right. (B) Profile of the LI along the dendritic shaft of GI 10-2. The magnitude of the LI at various locations is plotted along the dendritic shaft shown by a red line in the inset image. The horizontal axis indicates the anatomical distance from the point of intersection between the dendritic shaft and the midline. Gray lines correspond to individual LI profiles calculated from each measurement and the red line indicates the averaged value from 12 measurements in 10 neurons. Scale bars = 100 μm .

Fig. 1

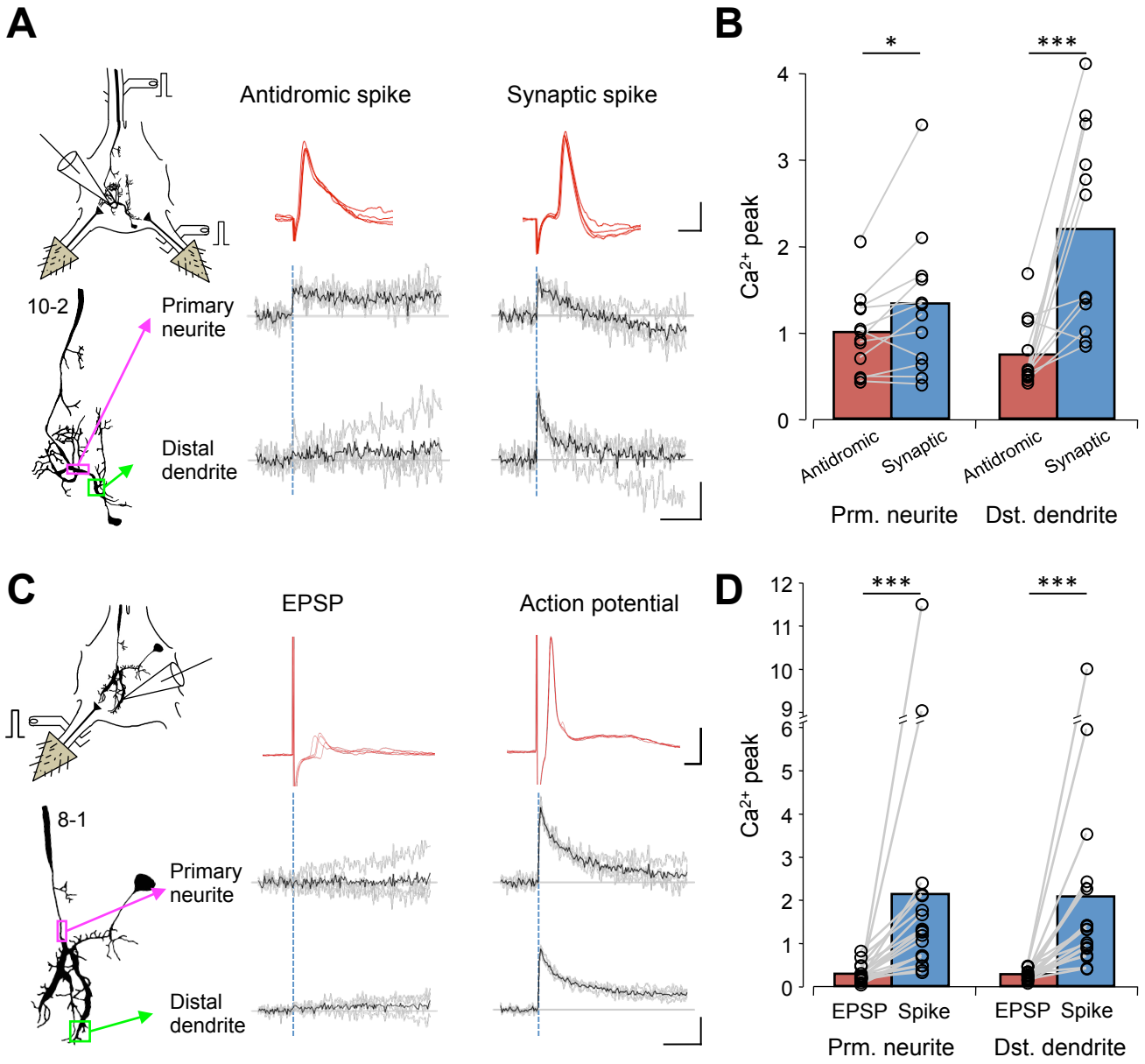


Fig. 2

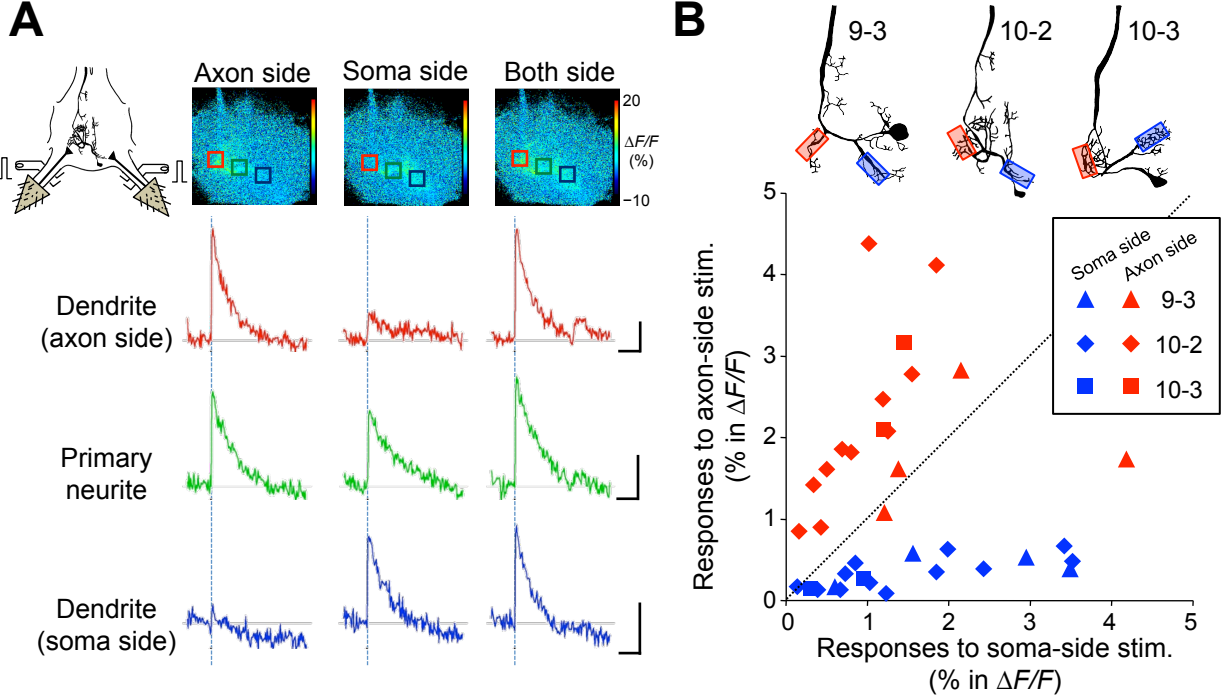


Fig. 3

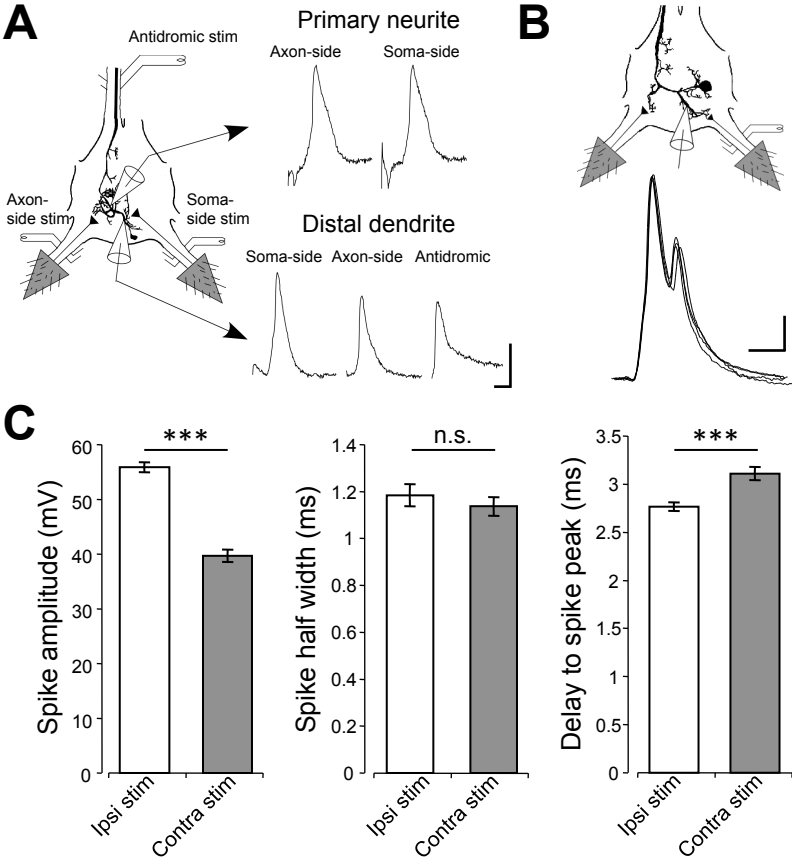


Fig. 4

